Journal of Renewable Materials

Tech Science Press

DOI: 10.32604/jrm.2022.018386

ARTICLE

Effect of Recycled Mixed Powder on the Mechanical Properties and Microstructure of Concrete

Chao Liu[1,2,*], Huawei Liu[2,*] and Jian Wu[1]

[1]Shaanxi Key Laboratory of Safety and Durability of Concrete Structures, Xijing University, Xi'an, 710123, China

[2]School of Civil Engineering, Xi'an University of Architecture and Technology, Xi'an, 710055, China

[*]Corresponding Authors: Chao Liu. Email: chaoliu@xauat.edu.cn; Huawei Liu. Email: liuhuawei@xauat.edu.cn

Received: 21 July 2021 Accepted: 15 September 2021

ABSTRACT

In this paper, recycled bricks and recycled concrete were applied to prepare eco-friendly recycled mixed powder (RMP) cementitious material, as a supplementary to replace conventional cement for improve the recycling of construction and demolition waste. Based on the effect of cementitious materials on the hydration of silicate cement, the effects of RMP on the workability, mechanical properties and microstructure of recycled mixed powder concrete (RMPC) with the different replacement ratios and the 8:4 and 6:4 mixing ratio of recycled brick powder (RBP) and recycled concrete powder (RCP) were investigated. The results showed that the fluidity of the mix decreased with increasing of the replacement ratio and the mixing ratio of RBP and RCP, but the influence of the fluidity was smaller within 15% replacement ratio. As the replacement ratio increases, the internal pore structure of RMPC tends to be loose and porous, which exhibits a significant pore volume distribution characteristic. The number of large capillaries was considerably increased at replacement ratio of 45%. The 7 d compressive strength of RMPC was slightly lower than that of ordinary concrete. The compressive and splitting tensile strengths of RMPC at 28 d increased by 4.2% and 10.1%, respectively, with increasing curing age at 15% replacement ratio and 6:4 mixing ratio. The RMPC mechanical strengths with RBP and RCP at the mixing ratio of 6:4 was higher than those of 8:2. Finally, a basis for the recycling of RBP and RCP in the construction industry can be provided by the results of this study.

KEYWORDS

Recycled concrete; recycled mixed powder; pore structure; mechanical properties

1 Introduction

With the rapid development of urbanization, a large amount of construction and demolition waste (C&DW), dominated by waste concrete and clay bricks, has been increased continuously [1–3]. In China, for instance, C&DW were generated at 1.6 billion and 1.8 billion tons in 2016 and 2017, respectively [4], and 5 billion tons are expected to be generated in 2021, with clay bricks comprising up to 50% [5]. However, the traditional way of C&DW disposal is mainly landfill, which not only fails to make full use of waste resources but also causes serious pollution of the environment and groundwater [6]. Therefore, it is imperative to propose a new and environmental-friendly way to dispose of a large amount of waste concrete and clay bricks [7].

Recycled brick powder (RBP) ground from waste clay bricks was found to have favorable volcanic ash activity [8,9]. The amorphous SiO_2 and Al_2O_3 in RBP reacted with the hydration product $Ca(OH)_2$ to form silicate and aluminate hydrates, and also the consumption of alkali content during the reaction helped to suppress the hazards caused by the alkali-silica reaction [10]. Lin et al. [11] argued that the early strength of concrete mixed with RBP developed slowly. However, with the increase of hydration time the volcanic ash activity of RBP gradually increased and a large number of gels were produced to improve the pore structure, therefore enhancing the late mechanical strength. The effect of RBP fineness on concrete strength was studied by Zheng et al. [12], and the results showed that the 28d compressive strength decreased by 4.25% when the RBP fineness was increased from 0.04 mm to 0.06 mm, and by 4.53% when the fineness was increased from 0.04 mm to 0.1 mm, under the condition that the RBP replacement ratio was 20%. Since the pozzolanic reaction and the compactness of the pore structure were promoted by the high-fineness RBP. Ma et al. [13] found that the mortar strength increased continuously with the increase of RBP at low incorporation, and the activity index of RBP reached the maximum at the incorporation of 10%, and the strength decreased rapidly after the incorporation over 10%. In summary, the mechanical properties of concrete generally decreased after the incorporation of RBP [8].

In addition to waste clay bricks, C&DW also contains a large amount of waste concrete containing coarse aggregates, and some scholars have conducted research on recycled concrete powder (RCP) obtained from waste concrete grinding [14–17]. Liu et al. [14,15] showed that the incorporation of RCP had no effect on the water requirement of cement standard consistency, and that RCP contains limestone powder with certain hydration activity to generate calcium monocarboaluminate with cement hydration products, which had no noticeable effect on the strength when RPC was mixed at less than 5%. In addition, the results of the literature [16,17] showed that the 28d compressive strength of mortar mixed with 15% RCP was increased by 30% and the bond strength by 6%, and the pore structure was refined and the compactness was improved compared to that of ordinary mortar. However, the volcanic ash activity of RCP is lower compared to that of the RBP, and the concrete mechanical strength decreases faster after the incorporation of RCP [8].

From above, it was found that RBP and RCP remained reactive. However, the effects of recycled mixed powder (RMP) mixed with as auxiliary cementitious materials to replace cement on the mechanical properties as well as microstructure of concrete have been rarely reported. Therefore, in this paper, the effects of RMP on the mechanical properties and workability of recycled mixed micronized concrete (RMPC) at different replacement ratios and mixing ratios were investigated by analyzing the microstructure and chemical composition of RMP. X-ray diffraction (XRD), mercury intrusion porosimetry (MIP) and scanning electron microscopy (SEM) were utilized to investigate the hydration properties and the microstructure evolution of RMPC, and the mechanism of the change of RMPC mechanical properties was revealed.

2 Materials and Methods

2.1 Materials

The cement used in the experiments was P·O 42.5 ordinary silicate cement. The fine aggregate was common river sand with an apparent density of 2.58 g/cm^3 and a fineness modulus of 2.62, and the grain size distribution is shown in Fig. 1. The coarse aggregate was 5–25 mm continuous graded crushed stone with an apparent density of 2.66 g/cm^3 and a crushing index of 10.6%.

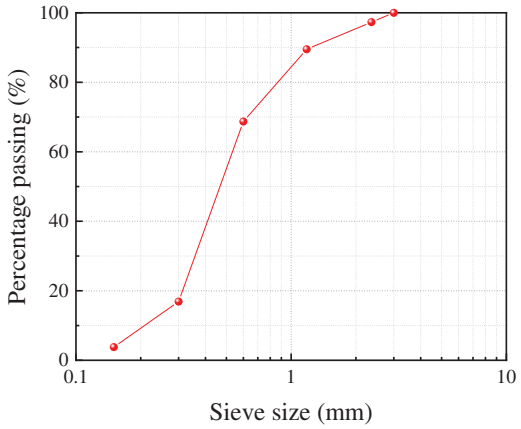

Figure 1: The grain size distribution of the fine aggregate

In this study, the RMP used consisted of RBP and RCP mixed with different mixing ratios. The recycled brick aggregate and recycled concrete aggregate used were purchased from Shaanxi Jian Xin Environmental Protection Technology Co., Ltd., China. To ensure the recycled brick aggregate and recycled concrete aggregate used were clean and not contaminated, the impurities were manually removed (such as mud). The jaw crusher type is HTHJK-125 × 150, feed size ≤ 80 mm, discharge size 5–25 mm. The ball mill type is horizontal ball mill, type 50–2000L, maximum feed size at 10 mm. The preparation process of RBP and RCP is divided into two steps due to the limitation of the ball mill for grinding objects at particle size: Firstly, waste clay bricks and concrete were initially crushed to the recycled coarse aggregate with the particle size of below 40 mm, and then secondly crushed to the recycled fine aggregate below 5 mm in particle size by the jaw crusher. Secondly, it was ground for different time periods by the ball mill. Finally, RBP and RCP particle size were controlled below 0.16 mm and mixed into RMP with different proportions. The preparation process is shown in Fig. 2. The physicochemical properties of cement, RBP and RCP are shown in Table 1. To study the effects of different RMP replacement ratios and mixing ratios on the concrete properties, RMP was substituted for cement by mass ratio at 0%, 15%, 30% and 45%, where the mixing ratios of RBP and RCP at 8:2 and 6:4, respectively, and the mix proportions of RMPC is shown in Table 2. The superplasticizer used in study was polycarboxylate superplasticizer with 20% water reduction rate. It should be noted that for simplicity of presentation, 8:2 and 6:4 means that the mass ratio of RBP and RCP is 8:2 and 6:4 in the following.

Table 1: Chemical compositions and physical characteristics of cement, RBP and RCP

Material	Mass fraction w/%							Specific surface area (m^2/kg)	Density (g/cm^3)	Water demand ratio (%)
	SiO_2	Al_2O_3	Fe_2O_3	CaO	K_2O	SO_3	MgO			
Cement	20.42	4.16	2.83	60.74	0.46	2.75	1.60	345	3.15	
RBP	63.47	17.51	8.26	1.84	2.85	0.13	1.19	424	2.62	104
RCP	30.20	7.81	3.05	42.66	1.43	0.45	2.14	457	2.56	103

Table 2: Mix proportions of RMP

Replacement ratio (%)	Mix proportion (kg/m^3)							
	Mixing ratio	Cement	RBP	RCP	Sand	Coarse aggregate	Water	Superplasticizer
0	0	370	0	0	610	1140	178	0.14
15	8:2	314.5	44.4	11.1				0.17
	6:4	314.5	33.3	22.2				0.16
30	8:2	259.0	88.8	22.2				0.25
	6:4	259.0	66.6	44.4				0.19
45	8:2	203.5	133.2	33.3				0.36
	6:4	203.5	99.9	66.6				0.29

Figure 2: Preparation process of recycled powder

2.2 Testing Method

2.2.1 Powder Particle Size Test

The particle size and particle size distribution of RBP and RCP powder were measured by LS230 laser particle size distribution analyzer, and the test range is 0.04–2000 μm.

2.2.2 Fluidity Performance Test

The slump was used to measure the fluidity of the mixture according to GB/T 50080-2016 "Standard for Test Methods for Performance of Ordinary Concrete Mixtures". The water demand ratio of RBP and RCP was tested by the standard GB/T 1596-2017 "Fly ash used in cement and concrete".

2.2.3 Mechanical Performance Test

According to GB/T 50081-2002 "Standard for Mechanical Properties of Ordinary Concrete Test Methods", the size of compressive and splitting tensile specimens was 100 mm × 100 mm × 100 mm, which were cured in the mold for one day after casting, and then demolded, cured at temperature (20 ± 2) °C and relative humidity ≥ 95% for 6 d and 27 d. Subsequently compressive and splitting tensile strength of the specimens were tested at 7 d and 28 d.

2.2.4 XRD

The phase transition of specimens was analyzed using the D/MAX2200 X-ray diffractometer of 2θ ranging from 15° to 70°. The samples were crushed and sampled, hydration was terminated with ethanol, dried at 40°C for 48 h to remove the internal moisture. Then samples were ground to less than 75 μm powder and analyzed the chemical composition of RMP at different mixing ratios by the XRD.

2.2.5 SEM

The microstructure of RMPC and RMP samples was observed by SEM. The type of SEM equipment used was Quanta 600 FEG, with a resolution of 1 nm and magnification from 100 to 400,000 times. The sample surfaces of 10 mm × 10 mm were obtained by cutting at a 1–2 cm position from the RMPC and RMP.

2.2.6 MIP

The characteristic of the pore structure was obtained by MIP tests. The type of the MIP used was Autopore IV 9500 with intrusion pressures ranging from 1.4 kPa to 414 MPa, corresponding to a pore diameter from 3 nm to 1000 μm. At the end of curing, each sample containing 4 g of particles was cut from the concrete.

3 Results and Discussion

3.1 Analysis of the Powder Particle Size, Chemical Composition and Micromorphology

The changes of the average particle size of RBP and RCP with the grinding time are shown in Fig. 3. With the increase of grinding time, the average particle size of RBP and RCP decreased rapidly in the first 30 min, but the average particle size decreased slowly in 30 min–50 min, and the grinding efficiency was low, and the average particle size decreased rapidly again after more than 50 min. In the meantime, the power consumption also increases with the increase of grinding time. To save energy and improve the efficiency of comprehensive utilization of C&DW. The grinding time RBP was 10 min and RCP was 30 min in order to satisfy the requirement that the both particle size ranging was from 0.5 to 100 μm.

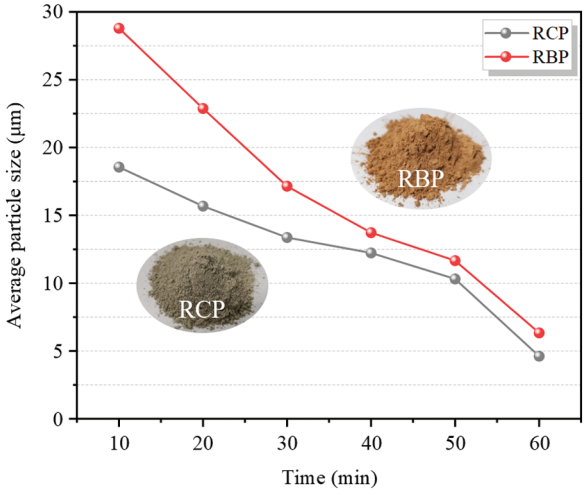

Figure 3: The average particle size of RBP and RCP varies with grinding time

The particle size distribution of RBP, RCP and cement are shown in Fig. 4. The median particle size, average specific surface area particle size, and average volume particle size of RBP were 18.56, 6.17, and 25.89 μm, respectively, and most of the particle sizes were within 25 μm. The median particle size, average specific surface area particle size, and average volume particle size of RCP were 17.15, 5.25, and

29.99 μm, respectively, and most of the particle sizes were within 65 μm. The average particle size of the cement is about 18 μm, which is slightly higher than the overall particle fineness of RBP and RCP. It has been reported [18] that the higher the content of particles size below 10 μm in fly ash, the higher the volcanic ash activity, while the volcanic ash activity is obviously reduced after the particle size is greater than 45 μm. In this experiment, the content of RBP and RCP particle size range below 10 μm was at 33.81% and 39.46%, respectively, and the content below 45 μm particle size range reached at 82.13% and 73.69%, respectively.

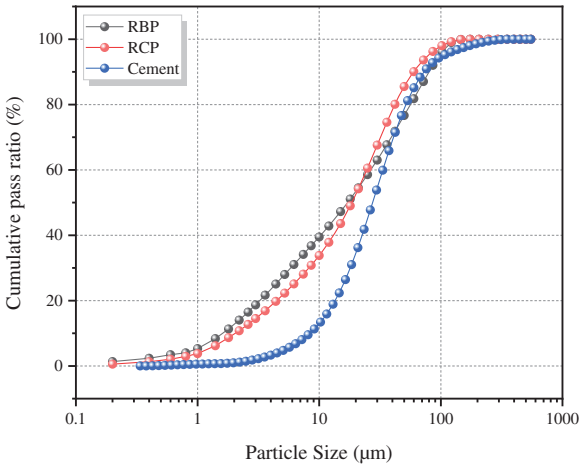

Figure 4: Particle size distribution of RBP, RCP and cement

According to the XRD results (Fig. 5), the main mineral composition of RBP is quartz (SiO_2), feldspar (feldspar), and hematite (Hematite). Calcite ($CaCO_3$), SiO_2, calcium hydroxide (CH), and not fully reacted C_2S, are the main mineral phases in the RCP. The higher intensity of SiO_2 characteristic diffraction peaks in RBP due to volcanic ash activity, calcium aluminate minerals in RCP and the higher intensity of $CaCO_3$ diffraction peaks are attributed to the cement nucleation effect can be facilitated. $CaCO_3$ can react with cement hydration products to form calcium aluminates, which can hinder the conversion of tri-sulfur type hydrated calcium thiosulfate (AFt) to monosulfur type hydrated calcium thiosulfate (AFm) and dense the pore structure of the mortar matrix [19].

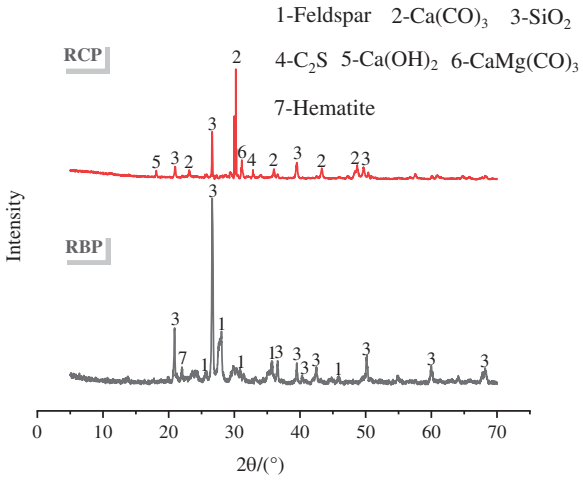

Figure 5: XRD patterns of RBP and RCP

The SEM images of RMP in Fig. 6 show that RMP particles are irregularly blocky and lamellar with rough morphology. The roughness of RMP at 8:2 mixing ratio is higher than 6:4, and its rough surface is beneficial to improve the adhesion with the mixed mortar [20], making it easier for cement to penetrate into RMP. It can be observed that the RMP particles have a destructive surface under high magnification, indicating that the particles contain internal mineral components that are prone to destructive processes. Furthermore, RMP can also be found to be loose and porous, containing microporosity inside, which can increase the internal frictional resistance between particles [21,22], which in turn affects the flowability of concrete during mixing.

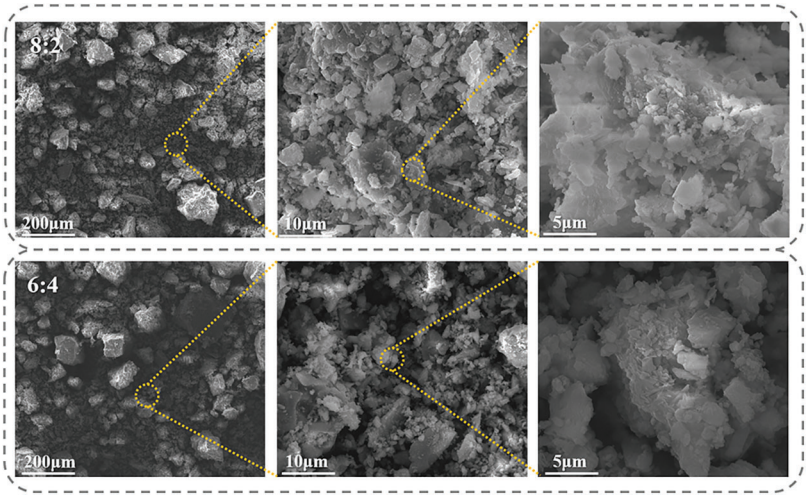

Figure 6: SEM images of RMP at different mixing ratios

3.2 Impact of RMP on Workability of RMPC

The amount of superplasticizer required to maintain the RMPC slump at 90 ± 10 mm for different mixing ratios is illustrated by Fig. 7 (the amount of water used in each group was kept constant, and the mixing time for each group was 5 min). The superplasticizer used increased with the increase of RMP replacement ratio. The amount of superplasticizer used at the mixing ratio of 8:2 was significantly higher than that of 6:4, which indicates that the flowability is reduced due to the incorporation of RMP, and the effect on flowability is greater with the increase of RBP mixing ratio. In addition, the more pronounced the porous characteristics inside RMP with RBP mixing (Fig. 6), this not only increases the water absorption, but also part of the mixing water and superplasticizer could be absorbed by these pores, causing a reduction in fluidity. However, the effect of fluidity at 15% replacement ratio was not remarkable.

3.3 Effect of RMP on Hydration Products

Fig. 8. shows the XRD patterns of specimens with different RMP incorporation at 28 d age (15° to 70°). It can be seen that the main phases of each specimen contain CH, calcium alumina (AFt), calcite ($CaCO_3$) and a small amount of incompletely reacted dicalcium silicate (C_2S), etc. Furthermore, new phases of white calcium zeolite ($2CaO\text{-}3SiO_2\text{-}2H_2O$) and calcium chalcocite (Ccn) were also generated. Compared with ordinary concrete, the intensity of CH characteristic diffraction peak in RMPC is weaker. The SiO_2 characteristic diffraction peak is pronounced because the reduction of cement content leads to decreased CH diffraction peak. At the same time, RMP also reacts with CH to produce gels such as C-S-H. The intensity of the CH diffraction peak after RBP incorporation is related to the degree of volcanic ash reaction of RBP. Compared with the mixing ratio of 8:2, $CaCO_3$ and the new phases of white calcium zeolite and calcium chalcocite diffraction peaks are raised at the mixing ratio of 6:4, which would

contribute to the generation of gels C-S-H and AFt and enhance the mechanical strength [23]. The SiO_2 diffraction peaks are gradually enhanced with the increase of RMP incorporation. In addition, the CH diffraction peaks are slightly changed at 30% and 45% replacement ratio of RMP. However, the intensity of the diffraction peaks of the new phase, $CaCO_3$, and AFt are weakened at different degrees, which indicates that the incorporation of RMP will obviously affect the generation of the new phase and the degree of its own volcanic ash reaction.

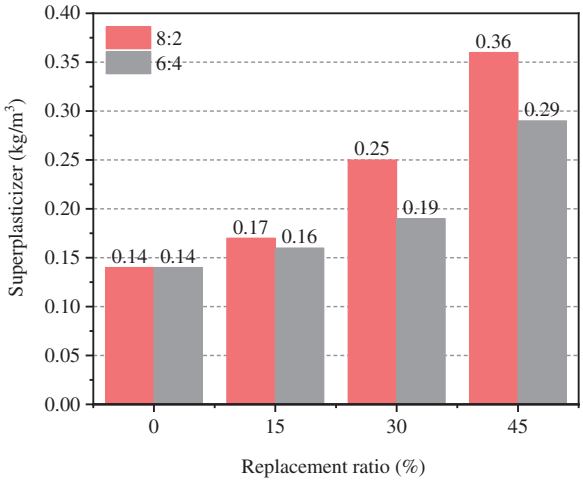

Figure 7: The relationship between RMP and superplasticizer consumption

3.4 Effect of RMP on Pore Structure

The porosity of specimens incorporated with RMP at different replacement ratios and mixing ratios is illustrated in Fig. 9. The porosity increases with the increase of replacement ratio, which indicates that the incorporation of RMP makes the internal pore structure loose and porous. On the one hand, this is because of its own porous properties, and on the other hand because the activity of RMP is lower than that of cement even though its fineness is finer than that of cement. The generation of hydration products is significantly reduced due to the large reduction of cement content at the replacement of 30% and 45%. Although RMP has volcanic ash activity, it is difficult to compensate for its own drawback of low reactivity and porous properties. As a result, the overall hydration reaction of the mortar was reduced, reducing the internal microstructure compactness and increasing the porosity. In addition, it was found that the porosity of specimens with 8:2 mixing ratio at the same replacement ratio condition was higher than that of 6:4, which also shows that a better hydration reaction can be obtained with the increase of RBP content compared to RCP.

The cumulative pore size distribution (PSD) of RMPC at different replacement ratios and mixing ratios is shown in Fig. 10. The rate of mercury intrusion is indicated by the slope of the curve, which reflects the number of pores at different pore sizes, and the larger the slope, the more pores in that pore size range. It can be seen that the pores were mainly distributed in the range of < 10 nm, 10 nm-100 nm, and close to 100000 nm. The overall PSD showed an increasing trend with the increase of RMP replacement ratio and was slightly higher than 6:4 for the specimens under the mixing ratio at 8:2. the cumulative PSD exhibited a remarkable growth at 45% replacement ratio compared with the other specimens.

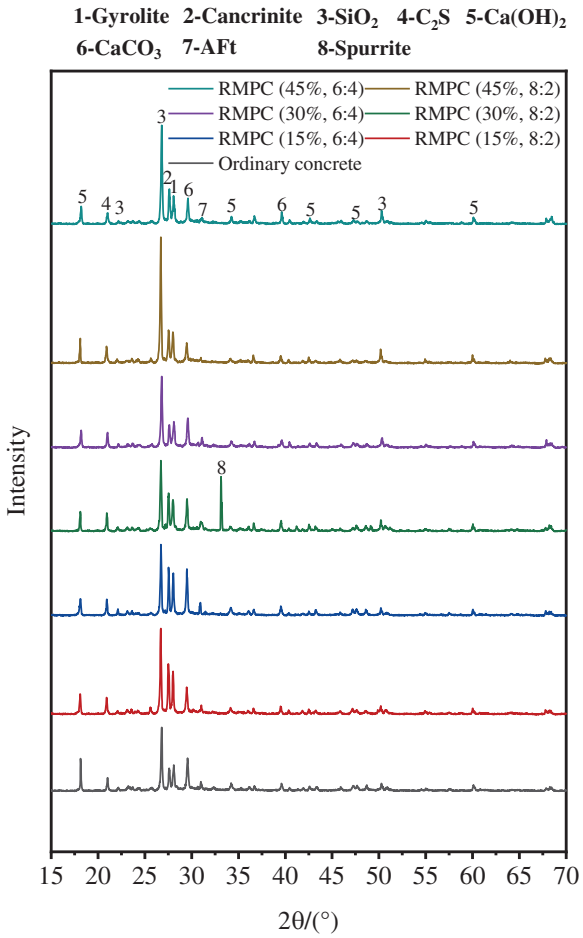

Figure 8: XRD patterns of RMPC at different RMP replacement ratios and mixing ratios

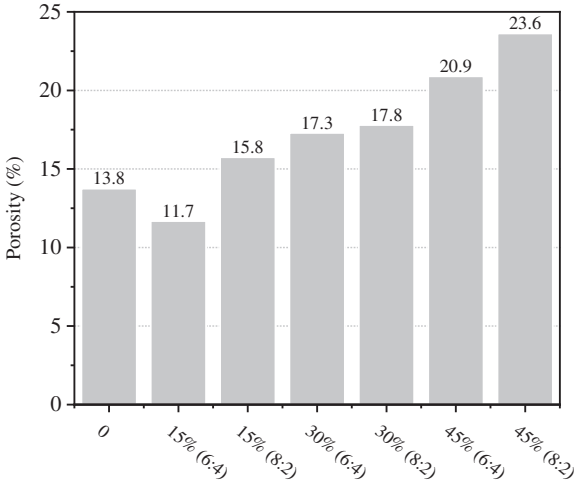

Figure 9: The porosity of RMP with different replacement ratios and mixed ratios

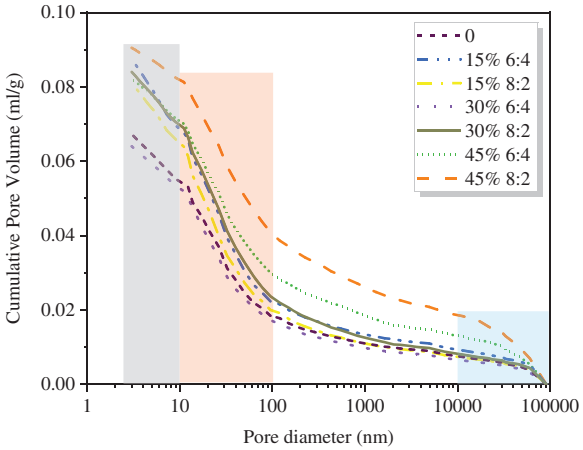

Figure 10: Cumulative pore size distribution at different replacement ratios and mixing ratios

For further in-depth analysis of the pore structure, the pore volume distribution (PVD) was further analyzed by dividing the pore diameter: gel pores (<4.5 nm), small capillary pores (4.5–50 nm), medium capillary pores (50–100 nm) and large capillary pores (100–100000 nm) [24] (Fig. 11). The results showed that significant PVD characteristics were exhibited. The pore volume of the specimens without RMP incorporation was mainly dominated by small capillary pores, followed by large capillary pores, and the volume proportion of the small capillary pores was larger than that of the large capillaries by 2.27 times. With the RMP replacement ratio increased, the proportion of small capillary pores and gel pore PVD decreased, the large and medium capillary pores increased. Compared to other pore volume types, the remarkable variation occurred in small and large capillary pores, especially at 45% replacement ratio.

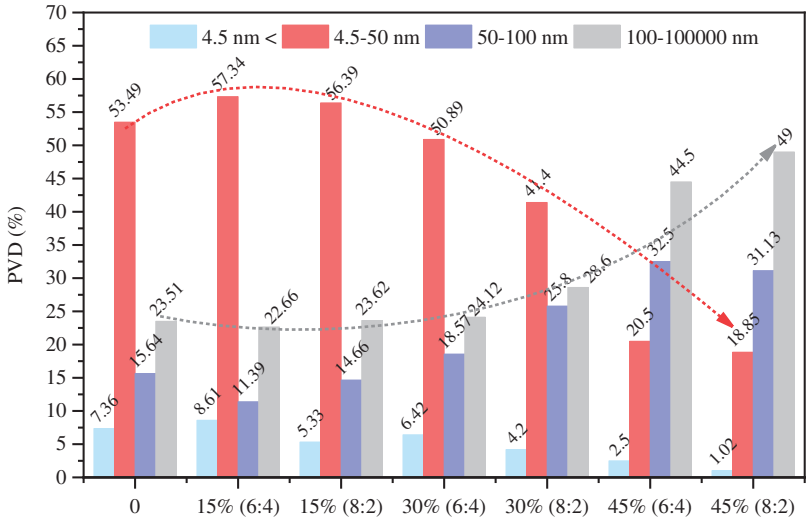

Figure 11: PVD for different pore size ranges

3.5 Analysis of Mechanical Property for RMPC

3.5.1 Compressive Strength

The compressive strength of RMPC showed a decreasing trend with increasing replacement ratio (except at 15% replacement ratio), and the strength decreased significantly when the replacement ratio was greater than 30%, as shown in Fig. 12a. Except for a slight increase at 15% replacement ratio, the strength loss in relative compressive strength was observed (Fig. 13).

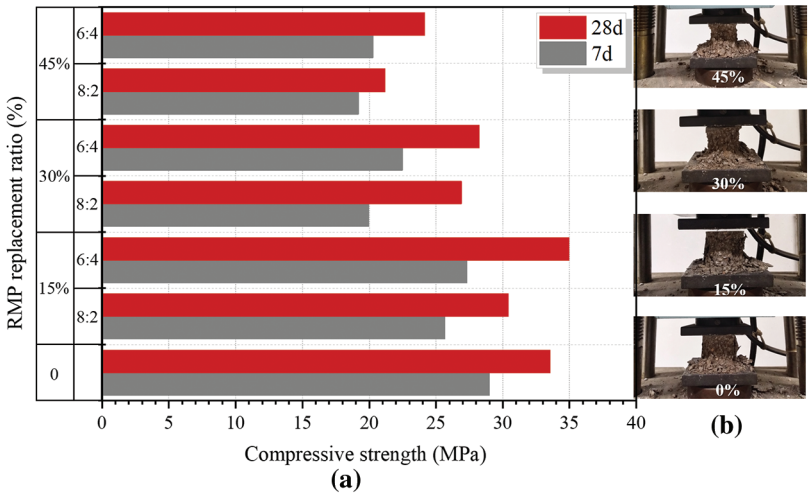

Figure 12: (a) Compressive strength of RMPC at different replacement ratios and mixing ratios. (b) Damage pattern of specimens at different replacement ratios (28 d) (RBP:RCP = 6:4)

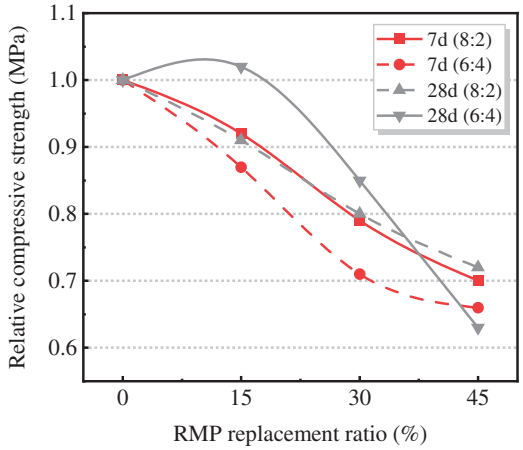

Figure 13: Relative compressive strength of RMPC at different replacement ratios and mixing ratio

The compressive strength of ordinary concrete specimens was highest at 7d and the higher the RCP incorporation the higher the strength at 28 d. The compressive strength of RMPC specimens (15%, 6:4) increased by 4.2% at 28 d but decreased by 5.8% at 7 d compared to ordinary concrete. At a mixing ratio of 8:2, the compressive strength at 7 d and 28 d was reduced by 11.5% and 9.4%, respectively, compared to ordinary concrete, and this difference in compressive strength decreased gradually with increasing age. This is mainly because the early volcanic ash activity of RMP was weak [25,26], with the physical filling

effect taking the dominant role, and less cementation products were generated by the reaction with the hydration product CH. With the increase of hydration age, the volcanic ash activity of RMP was reflected gradually. At the meanwhile, the mortar compactness was increased by the filling effect, because the RMP gradation was better at the mixing ratio of 6:4. In addition, on the one hand, the original hydration products in RCP can supplement Ca^{2+} for cement hydration reaction and play the role of crystal embryo to promote nucleation [27]. On the other hand, the effect of hydration nucleation can be excited by the aluminate phase in RBP [28]. Both RBP and RCP promoted the dual hydration effect at a suitable mixing ratio, thus the RMPC strength was increased after the cement was replaced by RMP at 15% replacement ratio. However, the compressive strength of RMPC was significantly reduced at 30% and 45% replacement ratios, which was attributed to a substantial reduction in cement, further reducing the generation of hydration products. However, the negative effect of cement reduction was not sufficient to be compensated by the filling effect and volcanic ash reaction of RMP.

The changes in the chemical reactions of the components caused by the different RMP replacement ratios and mixing ratios can be confirmed in RMPC by the variations in the pore structure parameters. In contrast to the pore structure characteristics of RMPC, the higher the porosity the lower the compressive strength in overall [8], and the compressive strength was inversely ratio to the volume proportion of small capillary pore and positively ratio to the volume proportion of large capillary pore. In other words, as the RMP replacement ratio and the mixing ratio of RCP and RBP increase, the compactness of the internal structural network of RMPC decreases, and therefore reduces the compressive strength. However, higher compressive strength can also be obtained if the replacement ratio and mixing ratio amount are reasonable, for example, specimen RMPC (15%, 6:4). In addition, it can be seen from Fig. 11b that as the RMP replacement ratio increases, the concrete of the specimens with 45% replacement ratio was sloughed the most when the specimens were crushed compared with the 30% replacement ratio, which is due to the highest proportion of the large capillary pores and loosening of the internal structure, resulting in poorer bond junction properties. In contrast, the 15% replacement ratio specimens showed no noticeable difference compared with the ordinary concrete specimens (The same vertical displacement control was applied to each specimen when it was damaged).

3.5.2 Splitting Tensile Strength

The splitting tensile strength results for RMPC were similar to the compressive strength, with an overall decreasing trend for RMPC as the replacement ratio increased, except for the specimens with a replacement ratio of 15% (8:2) (Figs. 14 and 15). Compared with the RMPC specimens (15%, 6:4), the splitting tensile strength was higher than that of ordinary concrete by 6.9% and 10.1% at 7 d and 28 d. In contrast, the splitting tensile strength of the specimens with a mixing ratio of 8:2 decreased by 4.2% and 6.3% compared with the ordinary concrete at 7 d and 28 d, respectively, which was attributed to the lower RCP content with smaller particle size, and influenced the RMP gradation distribution and activity.

RMP has physical filling and volcanic ash effect properties, which can have a “releasing effect” on cement hydration [29–31]. When cement is replaced by the RMP, the effective hydration component in cement was reduced, delaying CH crystallization and C-S-H nucleation [32], which affects early-age strength development by modifying the internal pore structure of RMPC. As the hydration proceeds, on the one hand, RMP gradually consumes the CH generated by the cementitious system through the volcanic ash effect, and also promotes cement hydration. On the other hand, the activity of RMP was activated by the freshly generated CH, making the hydration reactions between the cementitious materials to be promoted by each other [33]. Then new cementation products were continuously generated, which improved the microstructure and reduced the porosity inside the RMPC, and the bonding performance of the aggregate interface was enhanced. However, compared with ordinary concrete, the 28 d splitting tensile strength was reduced by 19.9% (8:2) and 8.0% (6:4) at 30% replacement ratio and by 23.6% (8:2)

and 18.3% (6:4) at 45% replacement ratio, respectively, which may be since a large amount of water was consumed by the volcanic ash reaction of RMP, resulting in insufficient water required for cement hydration and inhibiting the hydration effect [34]. Meanwhile, the concentration of Ca^{2+} was reduced by the large reduction of cement, reducing the generation of C-S-H and other gels, making the splitting tensile strength obviously to be lower.

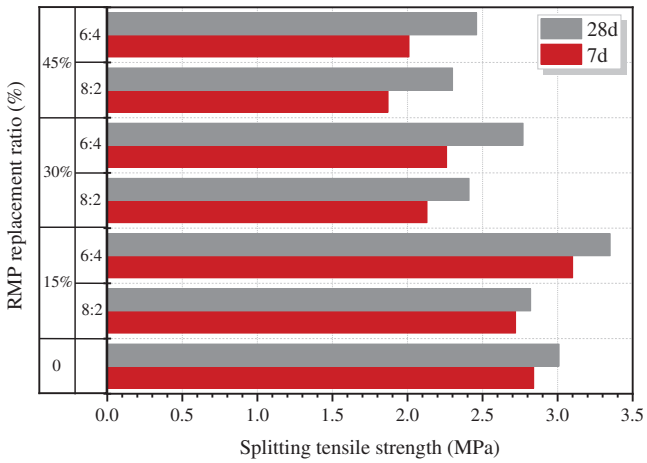

Figure 14: Splitting tensile strength of RMPC at different replacement ratios and mixing ratios

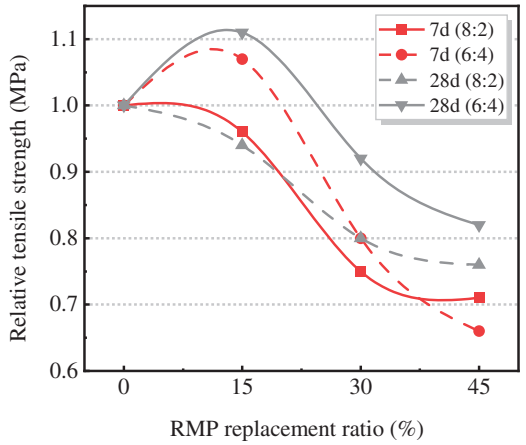

Figure 15: Relative splitting tensile strength of RMPC at different replacement ratios and mixing ratios

In terms of pore structure, the relationship between pore structure variations (porosity and PVD) and different RMP incorporation ratios for splitting tensile strength showed the same effect as that for compressive strength. Therefore, it can be concluded with certainty that RMP incorporation can influence the mechanical strength by modifying the pore structure characteristics.

3.6 Effect of RMP on Microstructure

It can be seen from Figs. 16a, 16b that the apparent appearance of the ordinary concrete is more loose and porous, and the compactness of the internal mortar structure of RMPC is higher than that of ordinary concrete, indicating that a certain physical filling effect is exerted by RMP [35] (this point is also can be

confirmed from the MIP test results). This effect is mainly manifested by the following two mechanisms: (1) Under the same water-binder ratio, increasing the contact ratio between water and clinker makes the space for hydration products in the clinker phase larger. (2) The nucleation sites of the hydration products can be provided by the surfaces of RBP and RCP with finer particle size.

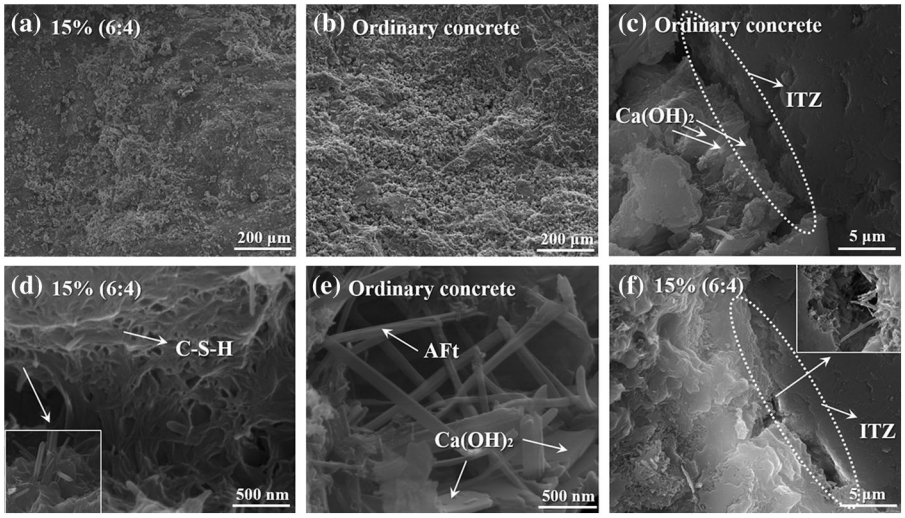

Figure 16: The microstructure of ordinary concrete and RMPC (15%, 6:4) at 28 d

Above, it was found that RBP has a certain pozzolanic activity during cement hydration, and RCP can conduct secondary hydration reactions with cement hydration products [36]. Since the water film could be attached to the surface of the aggregate, the water to cement ratio near the aggregate interface transition zone (ITZ) is often higher, and a larger crystalline product is formed. Therefore, a "weak skeleton" that is looser than the mortar matrix can be formed around the aggregate [8]. For ordinary concrete, CH is enriched in ITZ (Fig. 16c), and the uneven distribution of hydration products and the presence of connection defects at the interface lead to poor bonding between the mortar matrix and the aggregate in ITZ. For the RMPC, the "weak skeleton" can be filled with a large number of C-S-H, AFt and other gels generated due to the volcanic ash activity of RBP and the secondary hydration of CaO etc., in RCP with cement hydration products (Figs. 16d, 16e). This improves the compactness of the mortar matrix-aggregate interface (Fig. 16f) and inhibits the concentrated generation of CH at the aggregate interface, resulting in the strength of RMPC being improved. In addition, the surface of the RMP particles is rough and irregularly shaped, which facilitates the bond between mortar and aggregate, and therefore the adhesion of mortar in ITZ is improved [37]. On the other hand, the RMP with a loose and porous structure will absorb the water partially, which will reduce the effective water to cement ratio of concrete, and in turn increase the hardness of mortar and the compactness of ITZ. From the above analysis, it can be seen that the reason for the higher mechanical properties of concrete than ordinary concrete after incorporating the appropriate amount of RMP is explained by the difference between RMPC and ordinary concrete in microstructure and ITZ.

The number of the pores and cracks in RMPC significantly increased and the density of crystal clusters decreased with increasing RMP replacement ratio (Fig. 17). At the 30% replacement ratio, there were more pores inside the crystals and a small amount of hydration products AFt can be seen in Figs. 17c, 17d. Although the denseness of the mortar matrix and ITZ can be improved by the incorporation of appropriate amount of RMP, it is difficult to compensate for its porous properties and the inherent deficiency of low reactivity. Especially, at the RMPC with 45% replacement ratio, the degree of hydration reaction was drastically reduced, and less gel products were produced, which would generate a large

amount of lamellar CH and lead to the mortar matrix being looser (Figs. 17e, 17f). More importantly, the number of pores was significantly increased (Fig. 18a) and connected cracks appear within the pores in RMPC with 45% replacement ratio (Figs. 18b, 18c), and further observation reveals that there were also obvious micropores in the hydration products (Fig. 18d). This indicates that a large amount of RMP incorporation can reduce the degree of compactness as well as deteriorate the internal microstructure, decreasing the interfacial bond strength between the mortar and aggregate, and thus the overall strength of the cementitious system was reduced. As a result, the mechanical properties of RMPC were substantially reduced.

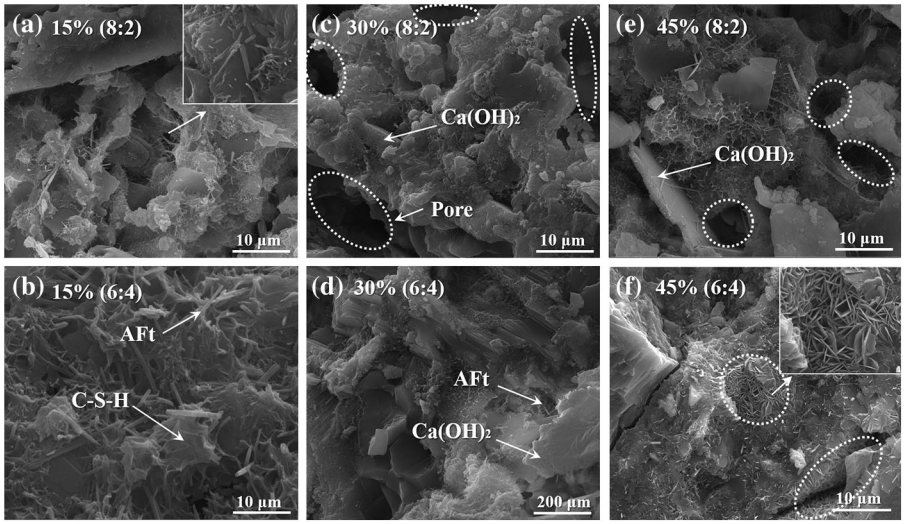

Figure 17: Effect of RMP replacement ratio on microstructure

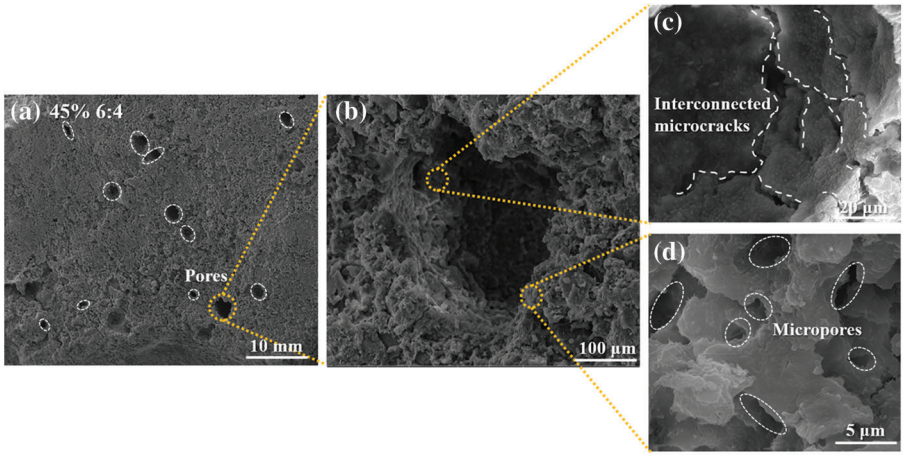

Figure 18: Microstructure of RMPC with 45% RMP replacement ratio

4 Conclusions

(1) The decrease in RMPC flowability after incorporation of RMP is attributed to the RMP particles with rough and porous and the high water absorption. The RMPC mix flowability is higher for RBP and

RCP mixing ratio of 6:4 than that of 8:2. There is no noticeable effect on RMPC flowability when the RMP replacement ratio is below 15%.

(2) The RMPC exhibited significant pore volume size distribution characteristics at different RMP replacement ratios. The pore volume increases with the increase of the replacement ratio. The PVD changed from a dominant small capillary pore distribution to a dominant large capillary pore distribution with increasing replacement ratios. The RMPC can obtain a denser pore distribution at 6:4 mixing ratio with the same replacement ratio.

(3) When RBP and RCP are mixed in the ratio of 6:4 can play a better role at filling effect and activity to improve the microstructural compactness of mortar matrix and ITZ.

(4) The early strength of RMPC is not affected significantly by the RMP incorporation. At RMP (15%, 6:4), the compressive strength of RMPC is increased by 4.2% and splitting tensile strength by 10.1% at 28 d compared with ordinary concrete. Although the compactness of mortar matrix and ITZ can be improved by the RMP incorporation (15%, 6:4), the mechanical properties of RMPC significantly decreased at 45% replacement ratio. Therefore, the cement is only suitable to be substituted by RMP at a reasonable range.

(5) RMP (15%, 6:4) can be used as a supplementary cementitious material to replace cement without impacting the qualities of the concrete. It is helpful to achieve sustainable development of the construction industry.

Funding Statement: The authors gratefully acknowledge the support of the Shaanxi Provincial Key Laboratory of Concrete Structure Safety and Durability Open Fund Project (XJKFJJ201904) and National Natural Science Foundation of China (51878546).

Conflicts of Interest: The authors declare that they have no conflicts of interest to report regarding the present study.

References

1. Amin, M., Tayeh, B. A., Agwa, I. S. (2020). Effect of using mineral admixtures and ceramic wastes as coarse aggregates on properties of ultrahigh-performance concrete. *Journal of Cleaner Production, 273,* 123073. DOI 10.1016/j.jclepro.2020.123073.
2. Saffar, D., Tayeh, B. A. (2018). Influence of pottery clay in cement mortar and concrete mixture: A review. *International Journal of Engineering and Technology, 7(20),* 67–71. DOI 10.14419/ijet.v7i4.20.25852.
3. Tayeh, B. A., Saffar, D., Alyousef, R. (2020). The utilization of recycled aggregate in high performance concrete: A review. *Journal of Materials Research and Technology, 9(4),* 8469–8481. DOI 10.1016/j.jmrt.2020.05.126.
4. Xiao, J. Z., Ma, Z. M., Sui, T. B. (2018). Mechanical properties of concrete mixed with recycled powder produced from construction and demolition waste. *Journal of Cleaner Production, 188,* 720–731. DOI 10.1016/j.jclepro.2018.03.277.
5. Shao, J. H., Gao, J. M., Zhao, Y. S. (2019). Study on the pozzolanic reaction of clay brick powder in blended cement pastes. *Construction and Building Materials, 213,* 209–215. DOI 10.1016/j.conbuildmat.2019.03.307.
6. Ma, A., Rn, A., Bat, B. (2020). Properties of self-compacting high-strength concrete containing multiple use of recycled aggregate. *Journal of King Saud University-Engineering Sciences, 32(2),*108–114. DOI 10.1016/j.jksues.2018.12.002.
7. Tayeh, B., Arafa, M., Alqedra, M., Shihada, S., Hanoona, H. (2017). Investigating the effect of sulfate attack on compressive strength of recycled aggregate concrete. *Journal of Engineering Research and Technology, 4(4),* 137–143.
8. Tang, Q., Ma, Z., Wu, H., Wang, W. (2020). The utilization of eco-friendly recycled powder from concrete and brick waste in new concrete: A critical review. *Cement and Concrete Composites, 114,* 103807. DOI 10.1016/j.cemconcomp.2020.103807.

9. Zhang, T. S., Yu, Q. J., Wei, J. X. (2012). Efficient utilization of cementitious materials to produce sustainable blended cement. *Cement and Concrete Composites, 34(5),* 692–69. DOI 10.1016/j.cemconcomp.2012.02.004.
10. O'Farrell, M., Sabir, B. B., Wild, S. (2006). Strength and chemical resistance of mortars containing brick manufacturing clays subjected to different treatments. *Cement and Concrete Composites, 28(9),* 790–799. DOI 10.1016/j.cemconcomp.2006.05.014.
11. Lin, K. L., Chen, B. Y., Chiou, C. S. (2010). Waste brick's potential for use as a pozzolan in blended portland cement. *Waste Management & Research, 28(7),* 647–652. DOI 10.1177/0734242X09355853.
12. Zheng, L. (2012). *Study on properties of waste clay brick powder concrete* (*Ph.D. Thesis*). University of Shan Dong, Jinan.
13. Ma, C. T., Song, J. X., Wa, C. B. (2009). Experimental study on utilization regeneration of powder of construction waste. *Ningxia Engineering Technology, 8(1),* 55–58. DOI 10.1177/1078155209104063.
14. Shi, C. J., Wang, D. H. (2017). Role of limestone powder and Its effect on durability of cement-based materials. *Journal of the Chinese Ceramic Society, 45(11),* 1582–1593 (in Chinese). DOI 10.14062/j.issn.0454-5648.2017.11.05.
15. Liu, S. (2010). Effect of limestone powder on hydration properties of composite cementitious materials. *Journal of Building Materials, 13(2),* 218–242 (in Chinese). DOI 10.1016/j.powtec.2020.11.029.
16. Brara, M., Be Brito, J., Veiga, R. (2014). Reduction of the cement content in mortars made with fine concrete aggregates. *Materials and Structures, 47(1–2),* 171–182. DOI 10.1617/s11527-013-0053-1.
17. Qin, L., Gao, X. J. (2019). Recycling of waste autoclaved aerated concrete powder in portland cement by accelerated carbonation. *Waste Management, 89,* 254–264. DOI 10.1016/j.wasman.2019.04.018.
18. Nuaklong, P., Jongvivatsakul, P., Pothisiri, T., Sata, V., Chindaprasirt, P. (2019). Influence of rice husk ash on mechanical properties and fire resistance of recycled aggregate high-calcium fly ash geopolymer concrete. *Journal of Cleaner Production, 252(5),* 119797. DOI 10.1016/j.jclepro.2019.119797.
19. Lu, D. Y., Zhang, S. H., Xu, J. T. (2017). Effects of limestone powder and metakaolin on strength and hydration assemblages of blended cements. *Journal of the Chinese Ceramic Society, 45(5),* 663–667 (in Chinese). DOI 10.14062/j.issn.0454-5648.2017.05.10.
20. Dang, J. T., Zhao, J. (2019). Influence of waste clay bricks as fine aggregate on the mechanical and microstructural properties of concrete. *Construction and Building Materials, 228,* 116757. DOI 10.1016/j.conbuildmat.2019.116757.
21. Lin, K. L., Wu, H. H., Shie, J. L. (2010). Recycling waste brick from construction and demolition of buildings as pozzolanic materials. *Waste Management & Research, 28(7),* 653–659. DOI 10.1177/0734242X09358735.
22. Zhao, Y. S., Gao, J. M., Liu, C. B. (2020). The particle-size effect of waste clay brick powder on its pozzolanic activity and properties of blended cement. *Journal of Cleaner Production, 242,* 118521. DOI 10.1016/j.jclepro.2019.118521.
23. Matschei, T., Lothenbach, B., Glasser, F. P. (2007). The role of calcium carbonate in cement hydration. *Cement and Concrete Research, 37(4),* 551–558. DOI 10.1016/j.cemconres.2006.10.013.
24. Metha, P. K., Monterio, P. J. M. (2006). *Concrete, microstructure, properties and materials.* McGraw-Hill, London.
25. Xue, C., Shen, A., Guo, Y. (2016). Effect of construction waste composite powder materials on the frost resistance of concrete. *Material Review, 30(2),* 121–125 (in Chinese). DOI 10.11896/j.issn.1005-023X.2016.04.029.
26. Perira-de-oliweira, L. A., Castro-gomes, J. P., Santos, P. M. S. (2012). The potential pozzolanic activity of glass and red-clay ceramic waste as cement mortars components. *Construction and Building Materials, 31,* 197–203. DOI 10.1016/j.conbuildmat.2011.12.110.
27. Sakai, E., Miyahara, S., Ohsawa, S. (2005). Hydration of fly ash cement. *Cement and Concrete Research, 35(6),* 1135–1140. DOI 10.1016/j.cemconres.2004.09.008.
28. Reig, L., Soriano, L., Borrachero, M. V. (2016). Influence of calcium aluminate cement (CAC) on alkaline activation of red clay brick waste (RCBW). *Cement and Concrete Composites, 65,* 177–185. DOI 10.1016/j.cemconcomp.2015.10.021.

29. Florea, M. V. A., Ning, Z., Brouwers, H. J. H. (2014). Activation of liberated concrete fines and their application in mortar. *Construction and Building Materials, 50,* 1–12. DOI 10.1016/j.conbuildmat.2013.09.012.
30. Lawrence, P., Cyr, M., Ringot, E. (2003). Mineral admixtures in mortars: Effect of inert materials on short-term hydration. *Cement and Concrete Research, 33(12),* 1939–1947. DOI 10.1016/S0008-8846(03)00183-2.
31. Cyr, M., Lawrence, P., Ringot, E. (2006). Efficiency of mineral admixtures in mortars: Quantification of the physical and chemical effects of fine admixtures in relation with compressive strength. *Cement and Concrete Research, 36(2),* 264–277. DOI 10.1016/j.cemconres.2005.07.001.
32. Kim, Y. J., Choi, Y. W. (2012). Utilization of waste concrete powder as a substitution material for cement. *Construction and Building Materials, 30,* 500–504. DOI 10.1016/j.conbuildmat.2011.11.042.
33. Narmiuk, M., Nawa, T. (2011). Effect of fly ash on the kinetics of portland cement hydration at different curing temperatures. *Cement and Concrete Research, 41(6),* 579–589. DOI 10.1016/j.cemconres.2011.02.005.
34. Liu, Q., Li, B., Xiao, J. Z. (2020). Utilization potential of aerated concrete block powder and clay br-ick powder from C&D waste. *Construction and Building Materials, 238,* 117721. DOI 10.1016/j.conbuildmat.2019.117721.
35. Lin, K. L., Wu, H. H., Shie, J. L. (2010). Recycling waste brick from construction and demolition of buildings as pozzolanic materials. *Waste Management & Research, 28(7),* 653–659. DOI 10.1177/0734242X09358735.
36. Kuma, M., Paul, J. M., Montero (2008). Microstructure, properties and materials of concrete. pp. 26–30. China Electric Power Press (in Chinese).
37. Liu, H., Liu, C., Bai, G., Zhu, C. (2020). Impact of chloride intrusion on the pore structure of recycled aggregate concrete based on the recycled aggregate porous interface. *Construction and Building Materials, 259(11),* 120397. DOI 10.1016/j.conbuildmat.2020.120397.